Fabrication of metal nanocluster and nanoparticles in the CaO-Bi2O3-B2O3-Al2O3-TiO2 glass by irradiation of XeCl pulsed laser

doi: 10.1364/OE.16.002614

Fabrication of metal nanocluster and nanoparticles in the CaO-Bi_2O_3-B_2O_3-Al_2O_3-TiO_2 glass by irradiation of XeCl pulsed laser

Hirokazu Masai*, Shintaro Mizuno, Takumi Fujiwara, Hiroshi Mori, and Takayuki Komatsu

[1]*Department of Applied Physics, Tohoku University 6-6-05, Aoba, Sendai, 980-8579, Japan*
[2]*Department of Materials Science and Technology, Nagaoka University of Technology 1603-1 Kamitomiokatyo, Nagaoka, 940-2188, Japan*
**Corresponding author: masai@laser.apph.tohoku.ac.jp*

Abstract: We report the fabrication of nanoparticles that contain metal nanoclusters at the surface of the CaO-B_2O_3-Bi_2O_3-Al_2O_3-TiO_2 glass using XeCl laser irradiation. We have demonstrated that the surface morphology such as that containing nanoparticles or a smooth flat surface can be controlled by laser irradiation conditions; the laser fluence, repetition rate, and temperature of the glass. The transmission electron microscope (TEM) images of the cross section of the nanoparticles show that the metal nanoclusters were formed inside the nanoparticle by XeCl pulsed laser irradiation, a unique phenomenon different from TiO_2-crystallization achieved by conventional heat-treatment of the glass. Since formation of nanoparticles containing metal nanocluster is a phenomenon different from previous papers about XeCl laser irradiation of oxide glasses, the combined process of pulsed laser irradiation and heat-treatment will open a wide variety of optical glass devices.

OCIS codes: (160.2750) Glass and other amorphous materials; (220.4610) Optical fabrication.

References and links

1. K. M. Davis, K. Miura, N. Sugimoto, and K. Hirao, "Writing waveguides in glass with a femtosecond laser," Opt. Lett. **21,** 1729-1731 (1996).
2. S. Maruo, O. Nakamura, and S. Kawata, "Three-dimensional microfabrication with two-photon-absorbed photopolymerization" Opt. Lett. **22,** 132-134 (1997).
3. M. Watanabe, S. Juodkazis, H.-B. Sun, S. Matsuo and H. Misawa, "Two-photon readout of three-dimensional memory in silica," Appl. Phys. Lett., **77,** 13-15 (2000).
4. W. Watanabe, T. Asano, K. Yamada, K. Itoh, and J. Nishii, "Wavelength division with three-dimensional couplers fabricated by filamentation of femtosecond laser pulses," Opt. Lett. **28,** 2491-2493 (2003).
5. M. Nogami, A. Ohno, and H. You, "Laser-induced SnO_2 crystallization and fluorescene properties in Eu^{3+}-doped SnO_2-SiO_2 glasses," Phys. Rev. B **68,** 104204/1-104204/7 (2003).
6. Y. Shimotsuma, K. Hirao, P. G. Kazansky, and J. Qiu, "Three-dimentional Micro- and Nano-fabrication in transparent materials by femtosecond laser," Jpn. J. Appl. Phys. **44,** 4735-4748 (2005).
7. T. Fujiwara, R. Ogawa, Y. Takahashi, Y. Benino, and T. Komatsu, "Laser-induced photnic periodic structure in tellrite based glass ceramics," Phys. Chem. Glasses, **43C,** 213-216 (2002).
8. H. Nishiyama, I. Miyamoto, S. Matsumoto, M. Saito, K. Fukumi, K. Kintaka, and J. Nishii, "Periodic precipitation of crystalline Ge nanoparticles in Ge-B-SiO_2 thin glass films," Appl. Phys. Lett. **85,** 3734-3736 (2004).
9. H. Nishiyama, I. Miyamoto, Y. Hirata, and J. Nishii, "Periodic structures consisting of germanium nanoparticles in buried channel waveguides," Opt. Express **15,** 2047-2054 (2007).
10. S. Mizuno, T. Fujiwara, Y. Benino, and T. Komatsu, "Novel Technique for Fabrication of Nanoparticle Structures in $KNbO_3$-TeO_2 Glass for Photonic Integrated Circuits," Jpn. J. Appl. Phys. **45,** 6121-6125 (2006).
11. H. Masai, S. Mizuno, T. Fujiwara, Y. Benino, T. Komatsu and H. Mori, "Creation of locally selective mirror surface on $40BaO$-$40TiO_2$-$20B_2O_3$ glass by XeCl pulse laser irradiation," J. Mater. Res. **22,** 1270-1274 (2007).

#90822 - $15.00 USD Received 12 Dec 2007; revised 28 Jan 2008; accepted 29 Jan 2008; published 11 Feb 2008

12. R. Sato Y. Benino, T, Fujiwara, and T, Komatsu, "YAG laser-induced crystalline dot patterning in samarium tellurite glasses," J. Non-Cryst. Solids **289,** 228-232 (2001).
13. T. Honma, Y. Benino, T, Fujiwara, T, Komatsu, and R. Sato, "Technique for writing of nonlinear optical single-crystal lines in glass," Appl. Phys. Lett. **83,** 2796-2798 (2003).
14. T. Honma, Y. Benino, T. Fujiwara, and T. Komatsu, "Transition metal atom heat processing for writing of crystal lines in glass," Appl. Phys. Lett. **88,** 231105-1-231105-3 (2006).
15. H. Masai, T. Fujiwara, and H. Mori, "Fabrication of TiO_2 nano-crystallized glass," Appl. Phys. Lett. **90,** 081907-1-081907-3 (2007).
16. N. Jiang, J. Qiu, and J. Silcox, "Precipitation of nanometer scale Zn crystalline particle in ZnO-B_2O_3-SiO_2 glass during electron irradiation," Appl. Phys. Lett. **77,** 3956-3958 (2000).
17. N. Jiang, J. Qiu, and J. C. H. Spence, "Precipitation of Ge nanoparticles from GeO_2 glasses in transmission electron microscope," Appl. Phys. Lett., **86,** 143112-1-143112-3 (2005).
18. I. Barin, F. Sauert, E. Schultze-Rhonhof, and W. S. Sheng, *Thermochemical data of pure substances part I and part II*, (VCH, Weinheim, 1989).

1. Introduction

Many studies on the local structural change of a glass matrix by laser irradiation have been reported with the progress in laser application technology [1-12]. Laser irradiation can induce a geometrically selective structural change, which is quite different from uniform bulk structural change caused by a conventional heating process using a furnace. If laser irradiation can induce a semi-permanent change in a glass matrix, such as change of refractive index or crystallization, these laser-induced changes provide unique properties without temporal decay. The crystallization, in particular, is a promising method for giving lightwave controllability, which is characteristic of crystal materials, because the created crystallites provide optical functions not achieved in conventional optical glass material. Thus, processed glass materials are expected to find application in optical function not achieved in conventional passive optical glass materials. There have been many reports on laser-induced change of a glass matrix by several kinds of lasers, such as ultra-fast (e.g. femto-second) pulsed laser [1-6], nano-second pulsed laser [7-11], or continuous wave (CW) laser [12-14]. However, there is a large difference between a femto-second laser and a nano-pulsed laser or a CW laser from the view point of the mechanism of laser-induced change in the irradiated material. The former can induce local changes with little thermal effect whereas the latter actively exploits the thermal effect for laser-induced change. Although femto-second lasers have high power density capable of inducing a structural change even in many transparent matrices, the phenomenon at the focus point of the laser beam is too complex to control. If we use the crystallization as a process for a functional glass, control of the thermal process should be necessary. Irradiation of glass materials with a laser having a thermal effect, therefore, is thought to be effective in preparing functional glass devices using controllable crystallization behavior. In using a thermal effect for a laser-induced structural change, the change depends on temperature and holding duration above the glass transition temperature. If we can control the temperature and a holding duration of the temperature, we can control the formation of crystallite nuclei or the growth of crystallites in stages, which is of great importance in creating tailored local structures. Irradiation with a CW laser adds a continuous photon energy which is converted into lattice vibration modes, and the temperature gradually increases above the glass transition temperature. On the other hand, nano-second pulsed lasers can serve peak power higher than CW lasers, bringing about rapid heating and cooling of the irradiated area. Thus, CW laser heating is similar to a very local furnace-heating whereas pulsed laser heating is momentary in nature, different from conventional furnace-heating. It follows that pulsed laser irradiation can induce unique structural change or crystallization at the surface, which has potential for fabricating novel optical devices.

Recently, Nishiyama et al. have succeeded in precipitating Ge particles in a GeO_2-B_2O_3-SiO_2 glass film by irradiation with a KrF laser followed by annealing at 600°C [8, 9]. The Ge particles were precipitated in the unirradiated area after heat-treatment. Since no precipitation

#90822 - $15.00 USD Received 12 Dec 2007; revised 28 Jan 2008; accepted 29 Jan 2008; published 11 Feb 2008

of metal particles was observed in a glass-ceramics obtained by a conventional heat-treatment using an electric furnace, the pulsed laser irradiation process has potential for fabrication of materials containing nanoparticles. Possible applications of materials containing nanoparticles include "plasmonics", the field for design and applications of surface plasmons in metal nanoparticles.

We selected the CaO-B_2O_3-Bi_2O_3-Al_2O_3-TiO_2 (CaBBAT) glass as the sample for irradiation with an excimer laser. Our group has already reported a selective crystallization of TiO_2 from the CaBBAT glass by a conventional heat-treatment [15]. Although it is difficult to attain a transparent crystallized glass containing TiO_2 crystallites because of refractive index mismatch between TiO_2 and the glass matrix, we have successfully obtained a transparent crystallized glass, in which the average diameter of TiO_2 crystallites was about 10 nm. The present pulsed laser irradiation experiment will shed light not only on the mechanism of the irradiation process but also on the process of the creation of the TiO_2-crystallized glass. In the present study, we examine the change at the surface of the CaBBAT glass after XeCl laser irradiation. The laser-induced morphological change is compared with a structural change induced by a conventional heart-treatment using an electric furnace.

2. Experimental

The CaBBAT glass was prepared by a conventional melt-quenching method using $CaCO_3$ (5 mol%), Bi_2O_3 (10 mol%), TiO_2 (20 mol%) and B_2O_3 (65 mol%). Batches were melted in an aluminum crucible (purity 99%) in an electric furnace at 1350°C for 40 min. The glass melt was quenched on a steel plate at 160°C, and then, annealed at the temperature of glass transition, T_g, for 30 min. The temperatures of glass transition, T_g, crystallization onset, T_x, and crystallization peak, T_p were measured by differential thermal analysis (DTA) operated at a heating rate of 10 K/min. We used a XeCl pulsed laser with full width half maximum (FWHM) of pulse width of 8 ns, and the laser intensity of 26 mJ/cm^2 respectively. The pulse shot number was fixed at 1000 shots and the pulse repetition rate was 10 Hz. An objective lens with a focal length of 150 mm was used to focus the laser beam to an irradiation area. The irradiation area was 1.77 mm × 3.54 mm (at 133 mJ/cm^2), 1.63 × 3.26 mm (at 156 mJ/cm^2), and 1.36 mm× 2.72 mm (at 225 mJ/cm^2). A sample holder with a heat controller was used for heat-assisted laser irradiation. The image of the glass surface was observed with an atomic force microscope (AFM). We used X-ray diffraction (XRD) and transmission electron microscope (TEM) to examine the crystallites in the glass matrix.

3. Results and discussion

The obtained transparent CaBBAT glass was vinous in color and the T_g, T_x, and T_p measured by DTA were 569°C, 623°C, and 640°C, respectively. Figure 1 shows the AFM images of the CaBBAT glasses after XeCl laser irradiation. The three columns and three rows show the temperature of the sample and the laser fluence, respectively. As shown in Fig.1, particle-like structures are observed as typified by the images for the conditions 300°C/133 mJ/cm^2 and room temperature/156 mJ/cm^2. Note that the irradiation area was much larger than the viewing area of the AFM observation and that no scanning of the laser beam was employed. The average particle diameter and specific surface area, which were estimated using a default calculation of the AFM program, are shown in the upper shown in the left and lower right corner of each AFM image, respectively. Since the particles were protuberant over the standard surface of the glass, formation of nanoparticles shows that a local volume expansion has occurred. We note that the average diameter of the particles increases with increasing temperature as well as the laser fluence. From Fig. 1, we can speculate a morphological conversion from nanoparticles to a flat smooth surface; the particles developed (see the image with 133 mJ/cm^2, 300°C), fused with each other (see the image with 225 mJ/cm^2, r. t.), and then, a flat smooth surface was formed (see the image with 156 mJ/cm^2, 300°C). The surface roughness of the laser-irradiated glass (225 mJ/cm^2, 300°C) is 0.7 nm, about 1/10 of the value after conventional mechanical polishing. It indicates that the smooth surface is due to local

#90822 - $15.00 USD Received 12 Dec 2007; revised 28 Jan 2008; accepted 29 Jan 2008; published 11 Feb 2008

melting by the laser irradiation as in a previous report [11]. Although the softening temperature is above the crystallization onset temperature, which is thought to be a precursor of crystallization, the XRD of the irradiated area shows a halo pattern with no peak corresponding to crystallized TiO_2.

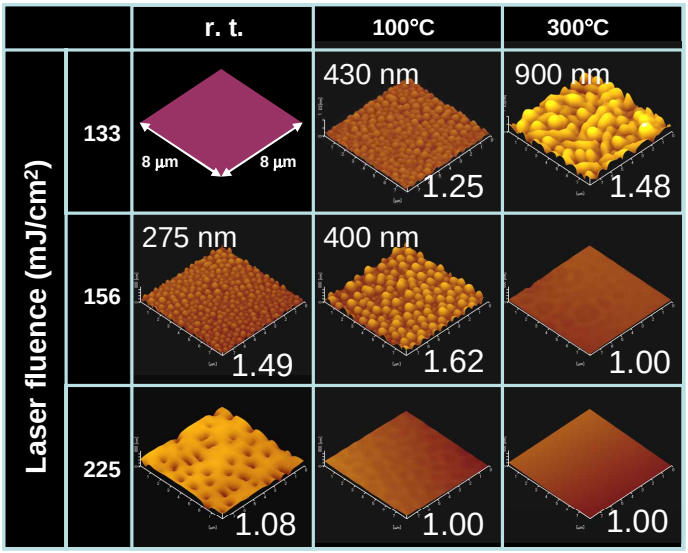

Fig. 1. AFM images at the surface of the CaBBAT glasses after XeCl pulsed laser irradiation. Three columns and three rows show the sample temperature and the laser fluence, respectively. The average particle diameter and specific surface area are shown in the upper left and lower right of each AFM image, respectively.

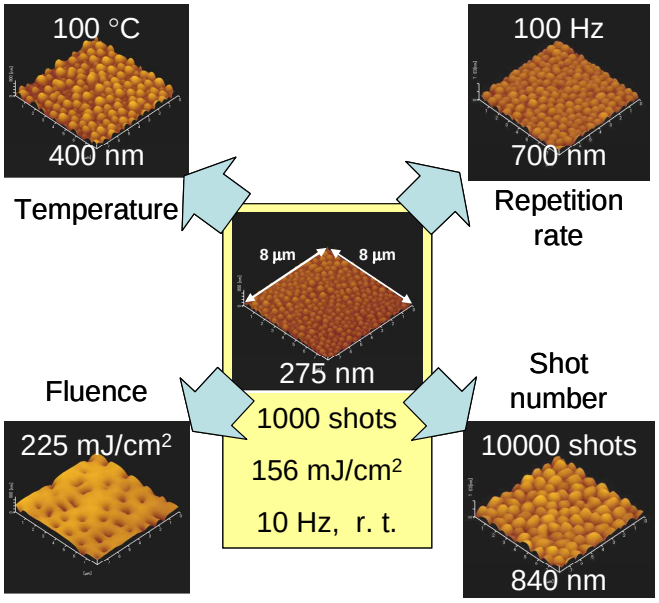

Fig. 2. AFM images at the surface of the CaBBAT glasses after XeCl pulsed laser irradiation with different irradiation conditions. The average particle diameter is shown in each AFM image.

#90822 - $15.00 USD Received 12 Dec 2007; revised 28 Jan 2008; accepted 29 Jan 2008; published 11 Feb 2008

Figure 2 shows an AFM image of the glass with different XeCl laser irradiation conditions. The center figure is an AFM image of the glass after laser irradiation at R.T. shown as a standard of irradiation condition. The shot number, laser fluence, and repetition rate of the irradiation were 1000 shots, 156 mJ/cm^2, and 10 Hz, respectively. The four surrounding images are the AFM images of the CaBBAT glasses with the same irradiation condition as the standard one except for one parameter shown in each figure. The particle size was affected by laser conditions: sample temperature, shot number, laser fluence, and repetition rate. Note that the average diameter of the particles after irradiation with 100 Hz-1000 shots or 10 Hz-10000 shots is larger than that of the standard sample. This indicates that an increase of repetition rate or shot number brought about an effect similar to sample heating and that not all the generated heat was dissipated within the interval of pulsed laser irradiation. It also indicates that the heat generated by laser irradiation accumulates in the glass matrix, which is a behavior different from the case of the $40BaO\text{-}40TiO_2\text{-}20B_2O_3$ glass that we have studied previously. In the case of $40BaO\text{-}40TiO_2\text{-}20B_2O_3$ glass whose T_g was 556°C, the average diameter of the particles at the surface was independent of the shot number [11]. Although the T_g of the $BaO\text{-}TiO_2\text{-}B_2O_3$ glass is similar to that of the present glass [11], the absorption coefficient at wavelength of 308 nm, thermal expansion coefficient, heat conduction coefficient are thought to be different for the two glass systems. The thermal properties of the glass, therefore, should be taken into account to explain the laser-induced phenomenon for a more detailed discussion.

Figure 3(a) shows an AFM image of the CaBBAT glass after XeCl laser irradiation through a phase mask with a 400 nm pitch. The laser fluence and sample temperature were 156 mJ/cm^2 and 90°C, respectively. Both the average particle diameter and the average interval between the tops of neighboring particles are both 400 nm, equal to the phase mask pitch. The standard deviation of particle size in a 400 μm^2 viewing area is less than 10 nm, which proves a high uniformity of the laser-induced particles. Since the surface was mechanically polished before laser irradiation, there are small scratches of nanometer scale at the surface of the sample remaining after irradiation. These small scratches are presumably the origin of the irregularity of the position and size of nanoparticle formation. Figure 3(b) shows the top view of the irradiated area.

Note that the laser-induced nanoparticles were generated densely resembling a hexagonal close-packing structure (Fig. 3(b)). Although the mechanism of this close-packing structure has not been clarified yet, the result shows that uniform and periodic nanoparticles can be fabricated on the surface of a glass by pulsed laser irradiation. For both manners of irradiation, with (Fig. 3) and without a phase mask (Fig. 1, 2), the sample system determines its particle

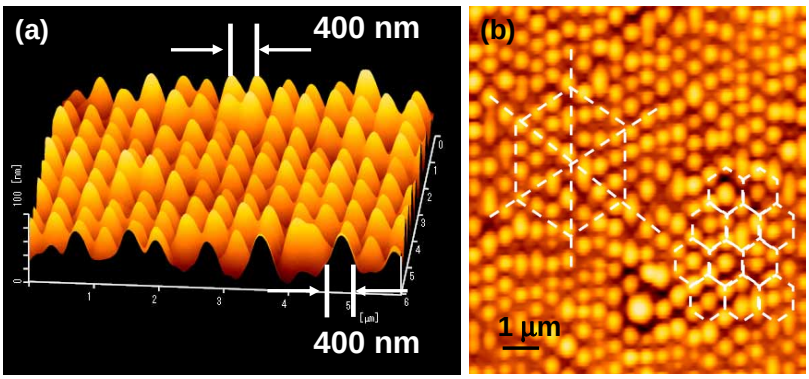

Fig. 3 (a) AFM images at the surface of the CaBBAT glasses after XeCl pulsed laser irradiation using a phase mask with 400 nm pitch. (b) The top view of the image.

#90822 - $15.00 USD Received 12 Dec 2007; revised 28 Jan 2008; accepted 29 Jan 2008; published 11 Feb 2008

diameter and inter-particle distance depending on the irradiation condition, namely, the particles are self-forming. For irradiation without a mask, no obvious long range order of particle positions is observed. For irradiation with a phase mask, the particles are aligned in the vertical direction due to the phase mask but a possible long range order is not obvious in the horizontal direction. Also noteworthy in Fig. 3 is the slightly elliptic shape of each particle with its long axis in the vertical direction, indicating that the particles are horizontally "squashed" by the constraint imposed by the mask pattern. This observation indicates that the self-formed diameter of the particles happens to be close to 400 nm, the mask pitch.

Figure 4(a) shows the TEM image of the cross section of a nanoparticle at the surface of the CaBBAT glass after laser-irradiation. The laser fluence and sample temperature were 156 mJ/cm^2, and 100°C, respectively. The white layer in the figure is an organic polymer film for surface coating. Figure 4(b) shows the TEM image of the cross section of an unirradiated area in the same sample. Although the precipitation of nanocrystallites induced by electron irradiation during the TEM observation with a strong electron beam was reported in other glass systems [16, 17], such precipitation was not observed in the present experiment.

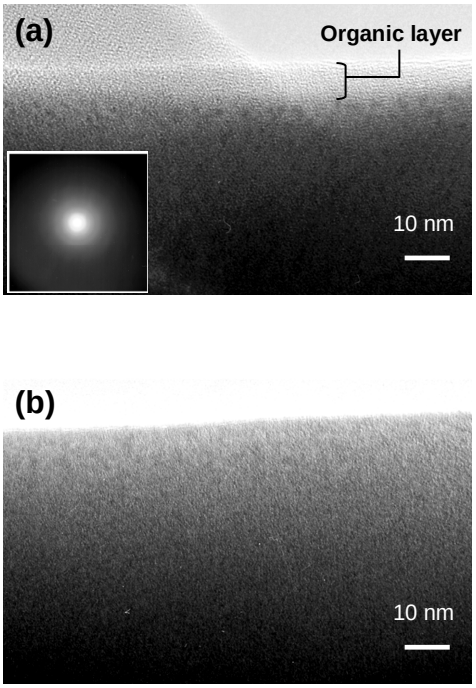

Fig. 4. (a) TEM image of the CaBBAT glass at the laser-irradiated area. (b) TEM image of the CaBBAT glass at an unirradiated area. Inset shows the electron diffraction pattern of the CaBBAT glass at an irradiated area.

In Fig. 4(a), many black dots with 1~2 nm diameter are observed near the surface of the glass, which leads us to conclude that the observed color contrast shows a difference of the electronic state; a light metal and a heavy metal. The observed thickness of crystallized layer was less than 20 nm. Since the electron diffraction image of Fig. 4(a) with no diffraction satellites indicates an amorphous state, we speculate that the black dots are nano-metallic clusters that are too small for analysis of the constituent cations by electron diffraction. Note that no such apparent dots, nano-metal clusters, are observed in Fig. 4(b). The present TEM images, therefore, show that the precipitation of the metal nanoclusters originates not from the strong electron beam but from the laser irradiation. Considering the chemical composition of the CaBBAT glass, the color contrast of the TEM image and the standard Gibbs free energy of

#90822 - $15.00 USD Received 12 Dec 2007; revised 28 Jan 2008; accepted 29 Jan 2008; published 11 Feb 2008

formation of M_xO_y (M = Ca, Bi, B, Al, and Ti) [18], it is speculated that these nanoclusters are attributed to bismuth metal clusters. Here we point out that no metal nanocluster was observed in the CaBBAT crystallized glass prepared by a conventional heat-treatment using an electric furnace, although the surface morphological change of the CaBBAT glass by laser irradiation also originates from the increased sample temperature. In the case of CW laser irradiation of a glass matrix, some oxides can be crystallized by a continuous energy supply [12-14] but no such metal crystallites have been reported. In a report by Nishiyama etal., they observed Ge metal particles precipitated in the unirradiated area of the glass film [8], which is opposite to the phenomenon observed in the present study. Their interpretation of the observation was that, in the case of the irradiation of a glass film via a periodic phase mask, the oxygen atoms in the unirradiated area move to the irradiated area to compensate the lost oxygen after irradiation, resulting in the formation of Ge nanoparticles in the unirradiated area. Our group reported the formation of nanoparticles, not metal clusters, at the surface of a TeO_2 glass after XeCl laser irradiation [7, 10]. On the other hand, uniform irradiation of the present bulk glass enhances the dissociation of the M-O (M : metal ion, O : oxygen) bond to form an M-M bond. It is speculated that a laser-induced photochemical reaction occurred to make metal nanoparticles in both cases. Since the present characteristic behavior of the laser irradiation process contains complex factors, not only thermal effects but also photochemical effects should be considered in future work.

6. Summary

In summary, we have fabricated a uniform distribution of nanoparticles at the surface of the CaBBAT glass by irradiation with a XeCl pulsed laser. The obtained result shows that a photochemical reaction as well as a thermodynamic reaction should be considered in the laser induced nanoparticle formation. The formation of metal nanoclusters in nanoparticles is a new result of XeCl pulsed laser irradiation to make functional materials. The present laser-irradiation process, coupled with the conventional heat-treatment, will open new application fields for functional optical devices.

Acknowledgments

This work was partially supported by the Grant-in-Aid for Scientific Research from the Ministry of Education, Science, Sport and Culture, Japan, and the research collaboration with Asahi Glass Co., LTD. The authors thank Dr. Takamichi Miyazaki and Dr. Kosei Kobayashi for taking the TEM images.

#90822 - $15.00 USD Received 12 Dec 2007; revised 28 Jan 2008; accepted 29 Jan 2008; published 11 Feb 2008